INDEPENDENT COMPONENT ANALYSIS OF NONSTATIONARY OSCILLATIONS DUE TO ROTOR BLADE FLUTTER

Boris Kukharenko
Department of Man-Machine Studies
Mechanical Engineering Research Institute RAS
Russia
kukharenko@imash.ru

Abstract

Collective unstable oscillations of rotor blades in case of flatter are under study. From a linear theory point of view, such unstable oscillations can consist of a single structural mode of blades. It has been found that flutter of real rotor blades can be two-modal: both torsion and bending mode excites simultaneously. As the collective oscillation amplitude increases, the flutter modes become nonlinear for all rotor blades simultaneously. Nevertheless, as usual, an analysis of respective simultaneous time-series is performed by a linear transform. In present paper it is the Independent component analysis (ICA). The linear ICA transform of multi-dimensional time–series under study displays that, as the rotation frequency increases, the rotor blade flutter evolves through four sequential time-phases: linear torsion flutter, nonlinear torsion flutter with bending mode excitation (torsion-bending flutter), linear bending-torsion flutter with a dominating role of bending mode, and nonlinear bending flutter of an unbounded amplitude increase with time.

Key words

Dynamic systems, structural modes, flutter.

1 Introduction

Collective unstable oscillations of rotor blades in case of flatter are under study. A central problem in oscillation record processing is finding a suitable representation or transform. As the collective oscillation magnitude increases, the flutter oscillation modes become nonlinear. Nevertheless, as usual, for computational and interpretation simplicity, an analysis of multi-dimensional oscillation time-series is performed by a linear transform. In present paper it is the Independent component analysis (ICA) [Hyvarinen, Karhunen and Oja, 2001]. ICA is a non-Gaussian version of factor analysis.

2 Independent component analysis (ICA)

Let $\mathbf{x} = (x_1,...,x_m)^T$ be a zero-mean m-dimensional random vector that is observed. The observed values of $\mathbf{x}$ correspond to a realization of m-dimensional discrete-time oscillation $\mathbf{x}(t)$, $t = 1,...,N$. (The fixed time-discretization step $\Delta t=1$ is selected for brevity). The ICA problem is to estimate the following data model:

$$\mathbf{x} = \mathbf{A}\cdot\mathbf{s} \tag{1}$$

where $\mathbf{s} = (s_1,...,s_n)^T$ is n-dimensional (hided) random vector, whose components are assumed to be mutually independent statistically, and $\mathbf{A}$ is a constant $m\times n$ matrix [Hyvarinen, Karhunen and Oja, 2001]. For linear transform of observed variable

$$\mathbf{s} = \mathbf{W}\cdot\mathbf{x} \tag{2}$$

constant weight matrix $\mathbf{W}$ is pseudoinverse of $\mathbf{A}$. As known, to identify model (2) independent components $\mathbf{s}$ must be non-Gaussian. The general formulation of ICA is based on the concept of mutual information. Differential entropy H of a random vector $\mathbf{s} = (s_1,...,s_n)^T$ with density $f(\mathbf{s})$ is defined as follows [Hyvarinen, Karhunen and Oja, 2001]:

$$H(\mathbf{s}) = -\int f(\mathbf{s}) \log f(\mathbf{s}) d\mathbf{s} \tag{3}$$

The differential entropy can be normalized to define the negentropy

$$J(\mathbf{s}) = H(\mathbf{s}_{\text{gauss}}) - H(\mathbf{s}) \tag{4}$$

where $\mathbf{s}_{gauss}$ is a Gaussian random vector of the same covariance matrix as $\mathbf{y}$. Negentropy J is invariant for linear transforms. It can be interpreted as a probability density measure to be non-Gaussian. The mutual information I, which constrains variables s_i, i=1,…,n to be uncorrelated, has the form

$$I(s_1, s_2, ..., s_n) = J(\mathbf{s}) - \sum_i J(s_i) \qquad (5)$$

So, ICA of a random vector $\mathbf{x}$ is an invertible transform, in which weight matrix $\mathbf{W}$ is determined so that the mutual information of components s_l is minimized. Since negentropy (4) is invariant for invertible linear transforms, it follows from (5) that finding weight matrix $\mathbf{W}$, which minimizes the mutual information, is equivalent to finding directions, in which the negentropy is maximized.

As shown in [Hyvarinen, Karhunen and Oja, 2001], some approximations of negentropy are more accurate than the approximations like kurtosis $\mathrm{kurt}(s_i) = E\{{s_i}^4\} - 3\left(E\{{s_i}^2\}\right)^2$. The simplest approximations have the form:

$$J(s_i) \approx c[E\{G(s_i)\} - E\{G(\nu)\}]^2 \qquad (6)$$

where G is a non-quadratic function, c is a constant, and ν is a Gaussian variable of zero mean and unit variance. So, random variable s_i is assumed to be of zero mean and unit variance also. The approximation (6) gives an objective function for estimating the ICA transform. So, to find one independent component $s_i = \mathbf{w}^T\mathbf{x}$, we maximize the function J_G given by

$$J_G(\mathbf{w}) = [E\{G(\mathbf{w}^T\mathbf{x})\} - E\{G(\nu)\}]^2 \qquad (7)$$

where $\mathbf{w}$ is an m-dimensional (weight) vector constrained so that $E\{(\mathbf{w}^T\mathbf{x})^2\}$=1. As it follows from (5), the mutual information is minimized, when the component negentropy sum is maximized.

As shown in [Hyvarinen, 1999] the functions $G(s)$ in (6), (7) are obtained by analyzing the exponential power family of density functions:

$$f_\alpha(s) = k_1 \exp(k_2|s|^\alpha) \qquad (8)$$

where α is a positive parameter, and k_1, k_2 are normalization constants that ensure $f_\alpha(s)$ to be a probability density of unit variance. For $0<\alpha<2$, eqs (8) gives a super-Gaussian density (i.e., a density of positive kurtosis). For $\alpha = 2$, eqs (8) gives the Gaussian distribution. For $\alpha > 2$, eqs (8) gives a sub-Gaussian density (i.e., a density of negative kurtosis). An optimal contrast function for estimating an independent component with density function $f_\alpha(s)$ has the form:

$$G_{\mathrm{opt}}(s) = a|s|^\alpha \qquad (9)$$

This implies that for super-Gaussian (respectively, sub-Gaussian) densities, the optimal contrast function grows slower than quadratic (respectively, faster than quadratic). Note that in practice most of independent components encountered are super-Gaussian. However, for $\alpha \le 1$ function (9) isn't differentiable at 0. Thus approximating differentiable contrast functions having qualitative behavior like (9) are in use. To maximize objective function (7) the ICA algorithm introduced in [Hyvarinen, 1999] is in use. The algorithm requires that the correlation matrix of $\mathbf{x}$ equals unity: $E\{\mathbf{x}\mathbf{x}^T\} = \mathbf{I}$. For one component, the maxima of $J_G(\mathbf{w})$ are obtained at certain optima of $E\{G(\mathbf{w}^T\mathbf{x})\}$. According to the Kuhn-Tucker conditions, the optima of $E\{G(\mathbf{w}^T\mathbf{x})\}$ under constraint $E\{(\mathbf{w}^T\mathbf{x})^2\}=\|\mathbf{w}\|^2=1$ are obtained at points, in which the condition holds

$$E\{\mathbf{x}g(\mathbf{w}^T\mathbf{x})\} - \beta\mathbf{w} = 0 \qquad (10)$$

where $g()$ is derivative of contrast function, β is evaluated as $\beta = E\{\mathbf{w}_0{}^T\mathbf{w}_0{}^T\mathbf{x}g(\mathbf{w}_0{}^T\mathbf{x})\}$, $\mathbf{w}_0$ is the value of $\mathbf{w}$ at the optimum. Eqs (10) is solved by Newton's method. To prevent converging to the same maxima, outputs $\mathbf{w}_1{}^T\mathbf{x},...,\mathbf{w}_n{}^T\mathbf{x}$ are uncorrelated after each iteration. Note that the algorithm performance has been estimated using different artificial mixes of test signals. A question is what would be results of the ICA separation for multi-dimensional natural piecewise linear/nonlinear non-stationary oscillations, for which their (time-dependent) spectral characteristics can be obtained reliably enough. Such example of multi-dimensional non-stationary oscillations is given by simultaneous oscillation records of rotor blades in case of flutter.

3 Collective unstable oscillations of compressor blades (flutter)

As a compressor rotation frequency increased, unstable blade oscillations can relate to two different phenomena: rotating stall and blade flutter. A whirl-type behavior like the rotating stall produces a sub-synchronous forward component of oscillations with frequency proportional to the rotation frequency [Bently, Goldman and Yuan, 2000]. But it is more important that, in case of the rotation stall, compressor blades oscillate independently. In contrast the flutter is a collective oscillation of compressor blades. Note that the theoretical study of flow-induced collective

bending-torsion oscillations of compressor blades shows: in the limit of uncompressed flow the torsion mode becomes unstable at first [Bendiksen, Friedmann, 1982]. Nevertheless, it is unknown, does the blade flutter is single-modal in real radial compressors, and what is a role of blade modes at various flutter time-phases.

The four low-frequency modes of compressor blades in case of flutter are well-known: 1st mode – 1st bending mode, 2nd mode – 1st torsion mode, and 3rd and 4th mode – modes compounded of 2nd bending and 2nd torsion [Gnesin, Bykov and Kovalev, 2000]. It gives an opportunity to place gauges on blade surfaces in locations of maximum magnitude of either 1st bending or 1st torsion mode. For compressor under study, simultaneous oscillation records $x_i = x_i(t)$, i=1,2,3 of three blades in a location of maximum magnitude of 1st bending mode are shown in Fig.1-3.

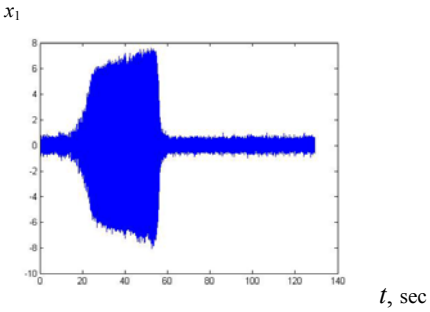

Fig.1. Oscillation record of 1st blade

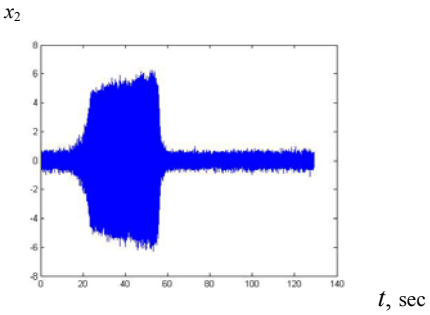

Fig.2. Oscillation record of 2nd blade

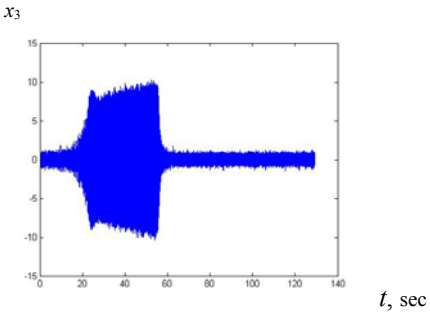

Fig.3. Oscillation record of 3rd blade

A rotation-frequency-time dependency of the compressor under study is shown in Fig.4.

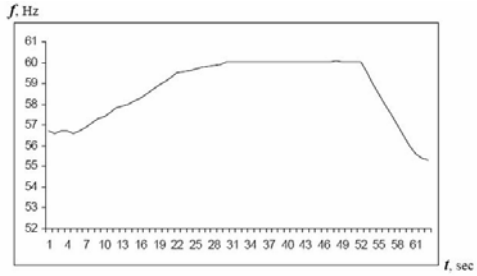

Fig.4. Rotation-frequency-time dependency of compressor

As shown in [Bendiksen, Friedmann, 1982], a flow-induced collective unstable oscillation of compressor blades (flutter) can be described by a liner model. It has been found that the flutter instability is related to an instant change of the damping factor sign of torsion mode. So, as the compressor blade oscillation magnitude increases (i.e., the flutter evolves in Fig.1-3), to define hide dynamic processes, both time-dependent natural frequency spectra and related time-dependent damping factor spectra must be obtained, especially times of instant changes of natural mode damping factors. As in [Kukharenko, 2002], to obtain time-dependent spectral parameters of oscillation records shown in Fig.1-3, the spectral analysis by Prony method is in use. A brief outline of the Prony method is given below. Let a segment of time-series (oscillation record)

$$x[k] = x((k\text{-}1)\Delta t),\ k = [1{:}N], \qquad (11)$$

where Δt – fixed time-discretisation step, represents time-dependency $x=x(t)$ of oscillation amplitude for $t\in[1,t_N]$, $t_N = N\Delta t$ (the time-series index is omitted, since each component of multi-dimensional time-series is processes individually by the Prony method). The time-series contains a noise, produced by a measurement incorrectness and non-stationary pulsations of gas flow. As above, Δt=1 is selected for brevity. The Prony spectral decomposition of segment (11) has the form:

$$x[k] = \sum_{l=1}^{p} r_l (z_l)^{k-1} + n(k)\ ,\ k = [1{:}N], \qquad (12)$$

where p – number of poles of segment (11); z_l=exp(δ_l+$j2\pi f_l$), l=[1:p] – segment poles where δ_l and f_l – respectively, damping factor and frequency; r_l=$A_l$exp($j\varphi_l$), l=[1:p] – residues in the poles where A_l and φ_l – respectively, amplitude and phase; $n(k)$ – additive noise. The method for determining number p of principal poles of segment (11) is presented in [Kukharenko, 2002]. As poles z_l,

l=[1:p] are determined, residues r_l, l=[1:p] in the poles are defined from (12) by the least-squares method. Note that main advantages of the Prony method algorithm in use are the opportunities: to select principal spectral components of segment (11) and to restore segment (11) theoretically by (12) with determined poles and residues. This gives an estimation of the Prony method exactness. The estimation of time-dependent damping factor and frequency spectra, and respective amplitude and phase spectra of the whole oscillation record is obtained by sequential shifts of a time-window of fixed length N. As the signal to noise ratio decreases, the Prony method algorithm demonstrates a high stability from computations point of view, especially for natural oscillation records. Note that natural oscillations are superposed of spectral components with coherent phases in contrast to artificial mixes of signals. Main results of spectral analysis of non-stationary oscillation records in Fig.1-3 are presented below.

The segmented spectral analysis of non-stationary time-series in Fig.1-3 shows how on basis of torsion oscillations of compressor blades (torsion flutter) collective unstable bending oscillations of blades (bending flutter) evolve.

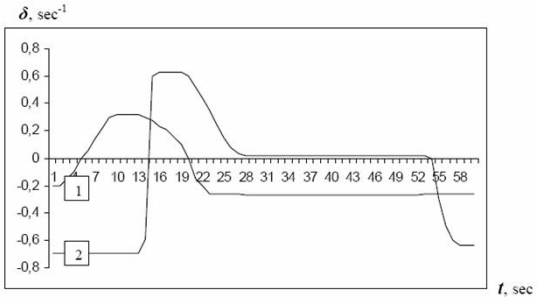

Fig.5. Damping-factor-time dependency for:
1 – 1st torsion mode; 2 – 1st bending mode

It has been found that the collective blade oscillation reflects in the similarity and simultaneous instant changes of damping-factor-time dependencies of bending and torsion mode (Fig.5) for 1st, 2nd, and 3rd blade of compressor. Thus, the time-dependent spectral parameters defined by the Prony method provide an opportunity to define simultaneous time-changes of blade modes for the radial compressor under study. Each time-series shown in Fig.1-3 consists of four successive time-segments, which differ in a shape of amplitude-time dependency. So, the time-series are representations of a single collective oscillation (flutter) of compressor blades.

4 ICA transform of collective unstable oscillations of compressor blades

The qualitative pattern of evolving collective oscillations of blades in Fig.5 is defined sequentially as result of a spectral analysis of each blade oscillation record. The segmented spectral analysis of each oscillation record is performed by sequential shifts of a time-window of fixed length. An advantage of the Independent component analysis is that all these records-representations of the collective blade oscillations are processed simultaneously and as whole. Processing non-stationary oscillation time-series $x_i(t)$, i=1,2,3 (Fig.1-3) shows opportunities provided by the Independent component analysis. It demonstrates also what kind of hide dynamic processes containing in these 3-dimensional time-series can be represented by components $s_i(t)$, i=1,2,3 (which are determined as mutually most independent). Note that respective independent components $s_i(t)$, i=1,2,3 wouldn't be blade natural modes, i.e. spectral components defined by the segmented Prony method. As noted the natural spectral components can be coherent in phase in time-superposition like natural oscillations. Independent components $s_1(t)$, $s_2(t)$, $s_3(t)$ separated by the ICA transform of oscillation time-series $x_1(t)$, $x_2(t)$, $x_3(t)$ are shown in Fig.6-8.

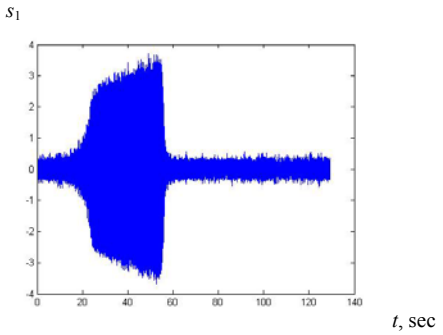

Fig.6. Time dependency of 1st component

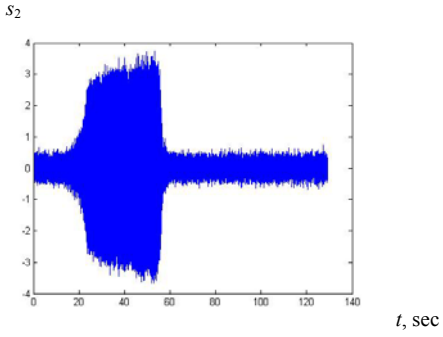

Fig.7. Time dependency of 2nd component

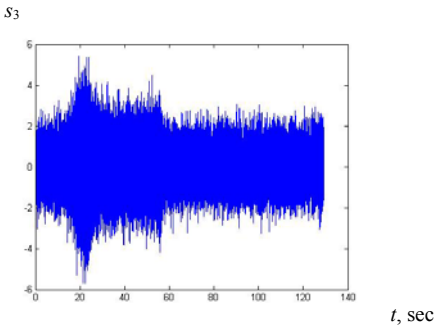

Fig.8. Time dependency of 3rd component

Mixing matrix **A** (1) and weight matrix **W** (2) has the value:

A =

-2.1830	0.2956	0.3378
-0.0132	-1.7616	-0.0983
1.2661	2.6323	0.6190

W =

-0.3297	0.2799	0.2243
-0.0461	-0.7051	-0.0868
0.8703	2.4260	1.5258

As it follows from matrix **A** and **W**, oscillation records $x_1(t)$, $x_2(t)$ play a role of signal-references, which provide an opportunity to separate independent component $s_3(t)$ in record $x_3(t)$ (so as in records $x_1(t)$, $x_2(t)$). Spectral analysis of components $s_1(t)$, $s_2(t)$, $s_3(t)$ by the segmented Prony method shows that their frequency spectra is similar to frequency spectra of observed oscillation records $x_1(t)$, $x_2(t)$, $x_3(t)$. However components $s_1(t)$, $s_2(t)$, $s_3(t)$ have different amplitude-frequency dependencies. By comparing with damping-factor-time dependencies of modes in Fig.5 it has been found that component $s_3(t)$ relates to the magnitude-time dependency of torsion mode. As result, the separation of independent components $s_1(t)$, $s_2(t)$, $s_3(t)$ of collective oscillation (its representations are shown in Fig.1-3) provides a qualitative pattern of flutter evolution. Oscillation records in Fig.1-3 evolve through four time-phases. In accordance with [Bendiksen, Friedmann, 1982], in 1st phase (t=[0;15]sec) the torsion flutter excites (δ_T>0 in Fig.5). For the compressor under study, the torsion flutter magnitude is bounded as a small difference exists between torsion frequencies of neighboring blades. In 2nd phase (t=[15;20]sec), the bending mode excites (δ_B>0 in Fig.5). The component $s_3(t)$ in Fig.8 has a maximum amplitude in time-interval $t\in$[17,4;20,3]sec, its frequency spectrum contains harmonics of the torsion frequency and the torsion mode is nonlinear. In 3rd phase (t=[20;25]sec), the torsion mode magnitude decreases (δ_T>0 in Fig.5) and the bending mode becomes dominant. Its amplitude increases with large positive damping factor until t≈25sec. At time t≈25sec (the deflection point of amplitude-time dependency of 1st component $s_1(t)$ in Fig.6) the torsion mode amplitude equals approximately its value at t=5sec, and damping factor δ_B of bending mode decreases instantly to ≈ 0.02 in Fig.5. At t≈25sec 4th final flutter phase starts. The amplitude of component $s_1(t)$ (Fig.6) is large enough, its frequency spectrum contains harmonics of the bending frequency, and the mode becomes non-linear. As shown in Fig.4, for time-interval $t\in$[0;25]sec, the compressor rotation frequency increases from 56.7 through 59.9Hz. Next, for time-interval $t\in$[25;54]sec the rotation frequency is constant approximately and equals ≈60Hz. At t=54sec, the rotation frequency decreases instantly to 55.5Hz. So, the flutter phenomenon exists in a narrow range of rotation frequency. Fig.9-10 show oscillation records x_4=$x_4(t)$ and x_5=$x_5(t)$ of two other blades of compressor under study in locations of the maximum magnitude of 1st torsion mode. The records in Fig.9-10 is similar to time-dependency of component $s_3(t)$ (Fig.8). Thus, the ICA transform of oscillation records $x_1(t)$, $x_2(t)$, $x_3(t)$ is equivalent to a separation (in each time-event) of space-superposition of the two 3D-forms of blade oscillation – bending and torsion (which exist mutually in maxima of each other). As result, time-dependency $s_3(t)$ is separated to be amplitude-time dependencies in another location, in which the torsion mode dominates.

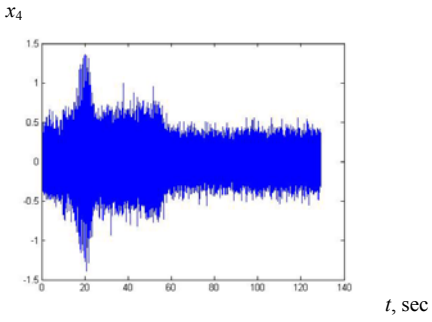

Fig.9. Oscillation record of 4th blade

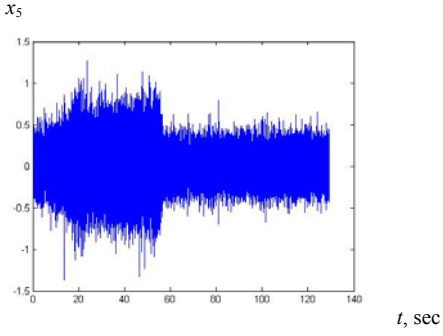

Fig.10. Oscillation record of 5th blade

The results of ICA transform of oscillation records $x_4(t)$ and $x_5(t)$ in Fig.9-10 shows, what hide dynamic processes are represented by their most independent components $s_4(t)$ and $s_5(t)$.

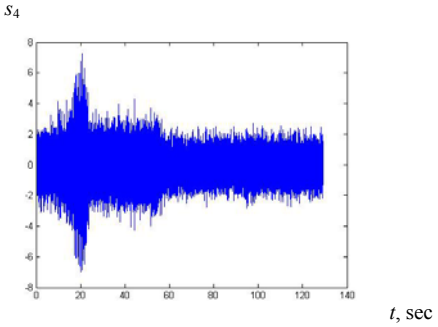

Fig.11. Time dependency of 4th component

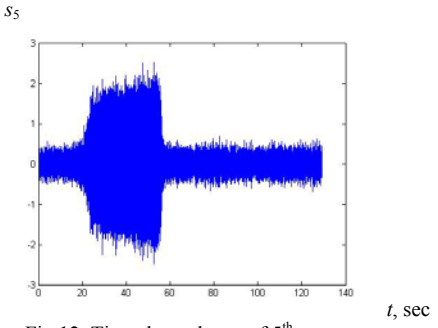

Fig.12. Time dependency of 5th component

Mixing matrix **A** (1) and weight matrix **W** (2) has the value:

A =

-0.1917	-0.0780
-0.0895	0.2054

W =

-4.4320	-1.6818
-1.9311	4.1353

As shown in Fig.11, independent component $s_4(t)$ represents the amplitude-time dependency in a location of the maximum magnitude of torsion mode. Other independent component $s_5(t)$ (Fig.12) represents the amplitude-time dependency in a location of the maximum magnitude of bending mode. This is similar to records shown in Fig.1-2. As noted, in case of flutter all blades oscillate similarly. So, different representations (Fig.1-3, Fig.9-10) of the blade collective oscillation are related to amplitude-time dependencies in respective locations on a single blade. In case of linear response of blade, the most independent components with respect to their amplitude-frequency dependencies are respectively, in locations of the maximum magnitude of 1st bending and 1st torsion mode [Dym, 1974]. In case of flutter these components are most independent also, as determined by the ICA transform (2).

5 Conclusions

The qualitative pattern of evolving rotor blade flutter can be obtained as result of the ICA transform of blade collective oscillation.

The linear ICA transform in time-domain can't replace a spectral decomposition in frequency domain.

References

Hyvarinen, A., Karhunen, J., and Oja, E. *Independent Component Analysis*. John Wiley & Sons. 2001.

Hyvarinen, A. Fast and Robust Fixed-Point Algorithms for Independent Component Analysis. *IEEE Transactions on Neural Networks.* 1999. **10**(3). p.p. 626-634.

Bently, D.E., Goldman, P., and Yuan, J. Vibrational diagnostics and rotor dynamics of centrifugal compressors in rotational stall. *Orbit*. Bently Nevada Corporation. 2000. **21**(1).

Bendiksen, O.O., Friedmann, P.P. The effect of bending-torsion coupling on fan and compressor blade flutter. *Transactions of the ASME*. 1982. **104**(3). p.p. 617-623.

Gnesin, V.I., Bykov, A.A., and Kovalev, A.S. Numerical simulation of flutter of blade cascades in inviscid gas flow. *Engineering Simulation*. 2000. **17**. p.p. 565-573.

Kukharenko, B.G. Spectral identification of periodic trajectories for the model of interwell jumps in a bistable oscillator. *Nonlinear Control Systems 2001* (A.L. Fradkov, and A.B. Kurzhanski, eds.) Oxford, Elsevier Science. 2002. **2**. p.p. 951-956.

Dym, C.L. *Introduction to the theory of shells*. Oxford, Pergamon Press. 1974.